CHAPTER 6

SIMONETTE REEF CASE STUDY

On the basis of conventional surface seismic data, the 13-15-63-25 W5M exploratory well was drilled into a low relief Leduc Formation reef (Devonian Woodbend Group) in the Simonette area, west-central Alberta, Canada. The well was prognosed to intersect the crest of the reef and to encounter about 50-60 m of pay; unfortunately, it was interpreted later to have intersected a flank position of the reef and was abandoned. The decision to abandon the well, as opposed to whipstocking in the direction of the reef crest, was made after the acquisition and interpretive processing of both near and far offset (252 and 524 m, respectively) vertical seismic profile (VSP) data, and after the reanalysis of existing surface seismic data.

The VSP survey was designed, performed and the results of a near and far offset VSP survey interpreted while the drilling rig remained on-site, with the immediate objectives of: (1) determining an accurate tie between the surface seismic data and the subsurface geology; and (2) mapping relief along the top of the reef over a distance of 150 m from the 13-15 well location in the direction of the adjacent productive 16-16 well with a view to whipstocking. These surveys proved to be cost effective in that the operator of the well was able to determine that the crest of the reef was out of the target area, and consequently that whipstocking was not a viable alternative. The use of VSP surveys in this situation allowed the owners of the well to avoid the costs associated with whipstocking, and to have confidence about their decision to abandon the well.

In this chapter, the 2-D surface seismic and VSP signatures of the low-relief reef in the Simonette study area (Hinds at al., 1993b and 1994c) are discussed with a view to obtaining a refined seismic image at the VSP-well and in the surrounding area . The 2-D data were acquired prior to drilling the 13-15 exploratory well which ultimately ended up intersecting the reef in a flank position below the oil/water contact as interpreted in this chapter. The initial processing of the raw VSP data was done by Vector Technology in 1987. The interpretive processing results presented in this chapter represent a more extensive treatment of all of the exploration data including the VSP data (taken from raw input data) and shown in Hinds et al (1993b).

6.1 Simonette Field

The Simonette Reef lies within the western Woodbend depositional realm (Stoakes and Wendte, 1987) where the reef environment is slightly different to that of the southeastern realm (Moore, 1989a). The southeastern realm included the geology for the case studies described in chapters 3 (Lanaway/Garrington field) and 4 (Ricinus field). A short review is presented below.

The Woodbend Group in central Alberta (Figs. 3.1A, B, and C) is subdivided into four formations: Cooking Lake, Duvernay, Leduc, and Ireton. In the Simonette study area of the western Woodbend depositional realm, the Cooking Lake Formation is depositionally absent and the Leduc Formation conformably overlies the Beaverhill Lake Group (Moore, 1989a).

The Leduc reef in the Simonette study area (Hinds et al., 1993b and 1994c) developed as both full and low-relief reef. The areal extent of the full reef which towers up to 230 m above the Beaverhill Lake platform, is defined roughly by the 70 m Ireton isopach contour interval in Figure 6.1. In Figure 6.1, the position of a geologic profile is shown defined by 8 wells with the corresponding geologic cross-section defined by the geophysical logs being shown in Figure 6.2.

Within the cross-section, well 10-34 penetrated the calcareous muds of the interior lagoon facies of the Leduc reef and was abandoned. Well 04-06 was drilled as a development well and is currently classified as an oil well although operations of producing from the well have been suspended. Well 10-06 was drilled into the northeastern portion of the Simonette atoll reef and is a flowing oil well. Well 04-16 was drilled into the raised peripheral rim (Anderson, 1986) and is a flowing oil well. The inter-reef well 10-16 was drilled off the rim of the main Simonette reef and penetrated only Ireton and Duvernay shales. Well 10-16 was abandoned. The five wells mentioned above were all drilled in the period 1960-62 when the Simonette Field was being developed in Alberta. Through numerous wells, the field was delineated and an Ireton isopach contour map (Hinds et al., 1993b) is shown in Figure 6.1 where the reef is interpreted to exist where the carbonates displace the encasing shales resulting in low shale isopach values.

Wells 16-16 and 04-22 were drilled in the period 1986-89 and are described in the next section. The final well shown in the geologic cross-section is the well 08-34 (a well in the shale basin) which did not encounter carbonate rocks of the Leduc Formation but was drilled through Ireton and Duvernay shales and Beaverhill Lake reef platform facies down to the Elk

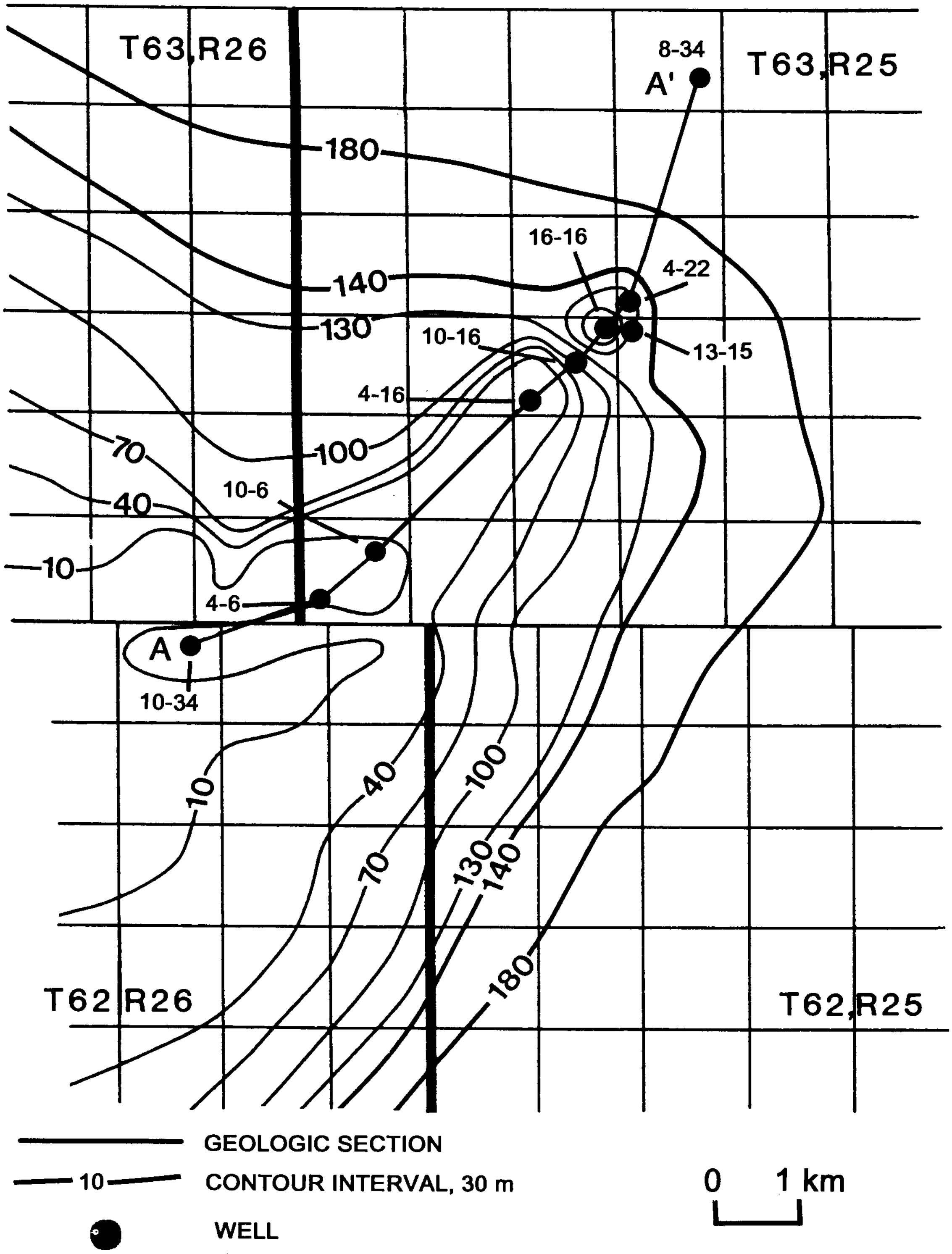

Figure 6.1 Ireton isopach map of the main and low-relief Simonette reef within the eastern Woodbend depositional realm. The locations of the wells used in the construction of the geologic cross-section shown in Figure 6.2 are shown in this figure. The exploratory well 13-15 is also posted (from Hinds et al., 1993b and 1994c).

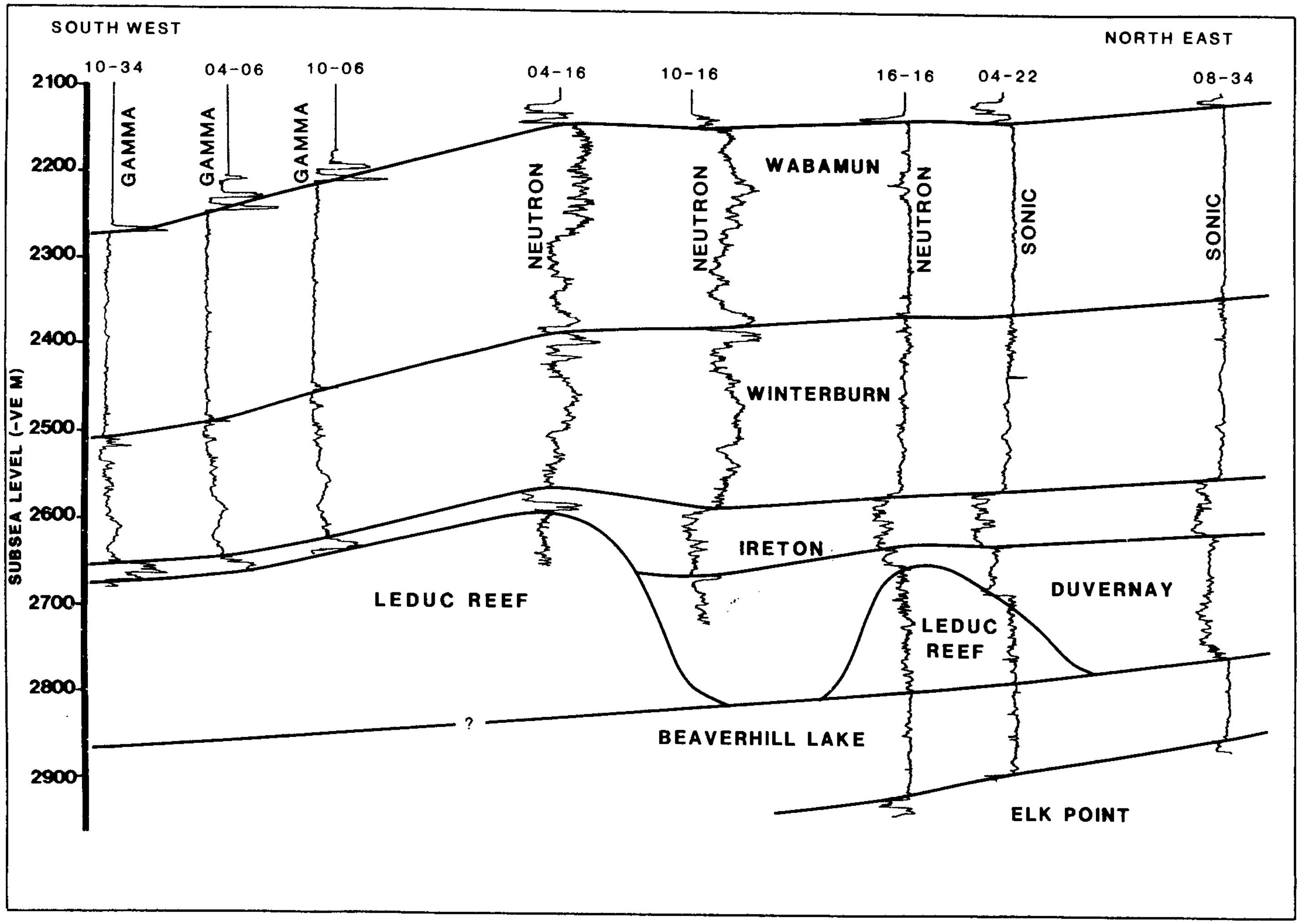

Figure 6.2 Geologic cross-section A-A' traversing the wells shown in Figure 6.1. The traverse starts in the southwest on the main Simonette reef at the back-reef lagoonal facies well, 10-34; continues to the northeast on the main reef for wells 4-6, 10-6, 4-16; into inter-reef shales for well 10-16; onto the low-relief reef with wells 16-16 and 4-22; and into the shale basin in well 8-34 (from Hinds et al., 1993b and 1994c).

Point Formation. The borehole logs within Figure 6.2 consist of neutron, gamma and sonic logs. The cross-section (Hinds et al., 1993b) shows the morphology of the Wabamun, Winterburn, Ireton, Leduc, Beaverhill Lake and Elk Point Formations and displays the placement of the study area reef (comprising of wells 16-16, 04-22 and the VSP-well, 13-15) with respect to the main Simonette atoll reef.

The low-relief reef of the study area, in contrast to the development of full reef buildup, attains a maximum thickness on the order of 120 m; its approximate areal extent is defined by the 130 m contour interval (Sections 15, 16, 21 and 22 of Township 63, Range 25 W5M; Fig. 6.1). The study area reef examined in this chapter is an isolated carbonate buildup that is basinward of the main Simonette atoll. The up-dip edges of both types of carbonate buildups can be productive where they are structurally closed and effectively sealed by the inter-reef shales of the Duvernay and Ireton Formations.

The term full reef was used in Anderson et al., (1989) to describe atolls and adjacent pinnacles which attain a height of over 200 m (Figs. 6.1 and 6.2) and is readily mapped on good quality 2-D seismic data; it is characterized by appreciable velocity pullup in the order of 30 ms, time structural drape of about 30 ms at the top of the Devonian (Wabamun Formation), and character variations within the Woodbend interval (the Leduc, Ireton and Duvernay Formation seismic events). The seismic signature of the low-relief reef which was the target of the VSP-well, as evidenced by the example seismic data (Fig. 6.3), is more subtle, being manifested by less than 15 ms of pullup and less than 15 ms drape of the Wabamun event from reef to off-reef. In addition, the reflection from the top of the low-relief reef can be difficult to distinguish from the Z-marker (an inter-reef shale event used

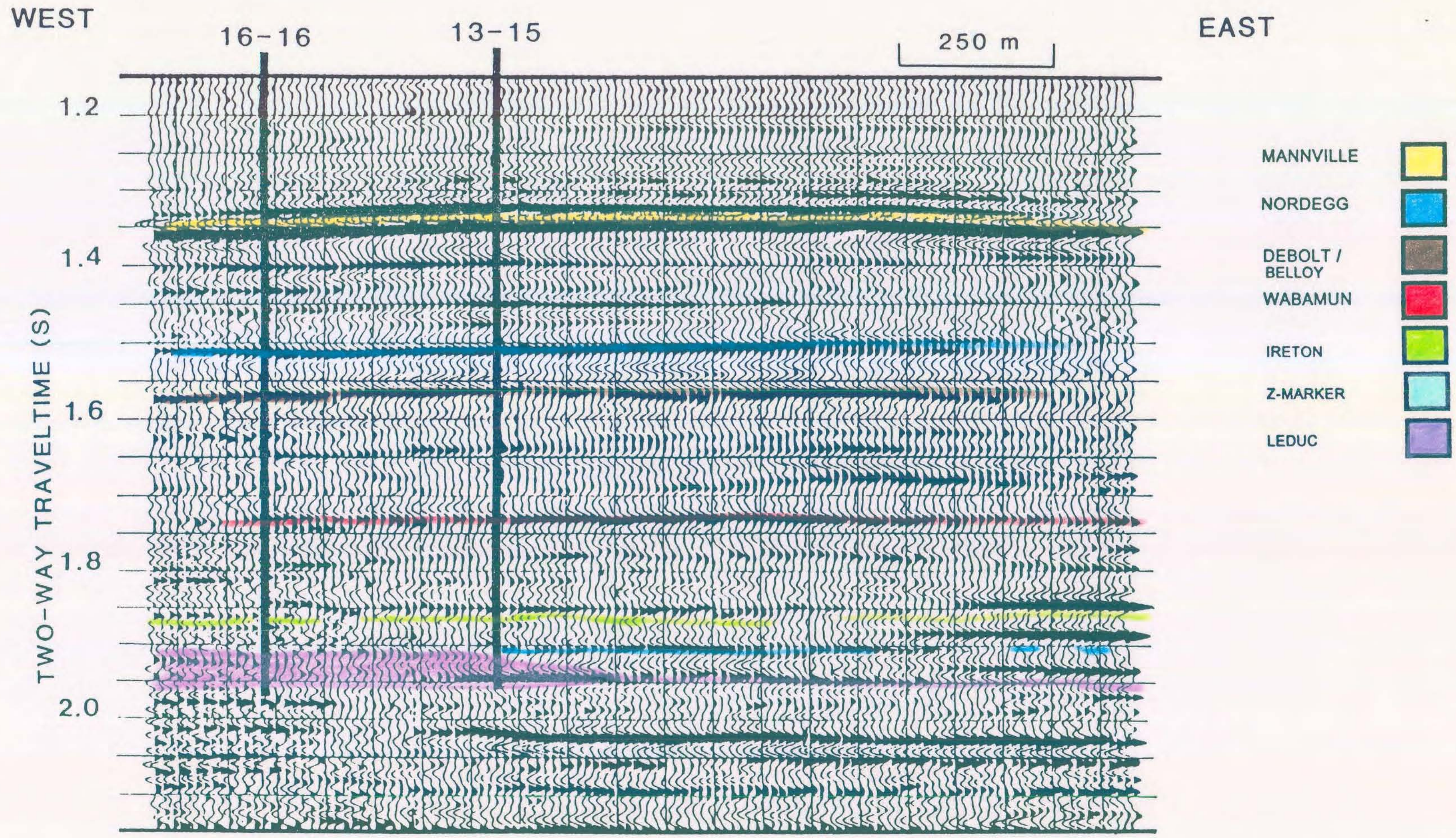

Figure 6.3 Example surface seismic data over the low-relief reef displaying the original interpretation of the owner of the data. The interpretation was done prior to the drilling of the well (from Hinds et al., 1993b and 1994c).

in the interpretation of seismic data in the Simonette atoll area; Hinds et al., 1993b). On Figure 6.3, an event beneath the reef at 2.2 s "pulls up" starting 8 traces East of the 13-15 well location (as shown on Fig. 6.3). This pullup suggested that the edge the low-relief reef could be located as indicated in Figure 6.3.

6.2 Simonette low-relief reef

Three wells penetrate the low-relief carbonate buildup seen as a northeast extension of the main Simonette reef in Figure 6.1; namely, 16-16-63-25 W5M, 4-22-63-25 W5M, and 13-15-63-25 W5M. Well 16-16 encountered 72 m of net pay; well 4-22 encountered 24 m of net pay but watered out after 12 months of production; well 13-15 is the abandoned exploratory well for which the two VSPs were acquired (see Fig. 6.4 for the three well locations).

The contour map of the Ireton to Leduc isochrons which was derived from the originally interpreted seismic data (interpreted by the owners of the seismic data) is shown in Figure 6.4. The prognosis was that well 13-15 would encounter 50-60 m of net pay. The contour map of Figure 6.5 summarizes the final preferred evaluation derived from the thesis work for the 13-15 location using the drilling results, the interpretation of the near and far offset nondeconvolved and deconvolved VSP data, and the reinterpretation of the suite of existing surface seismic lines within the area.

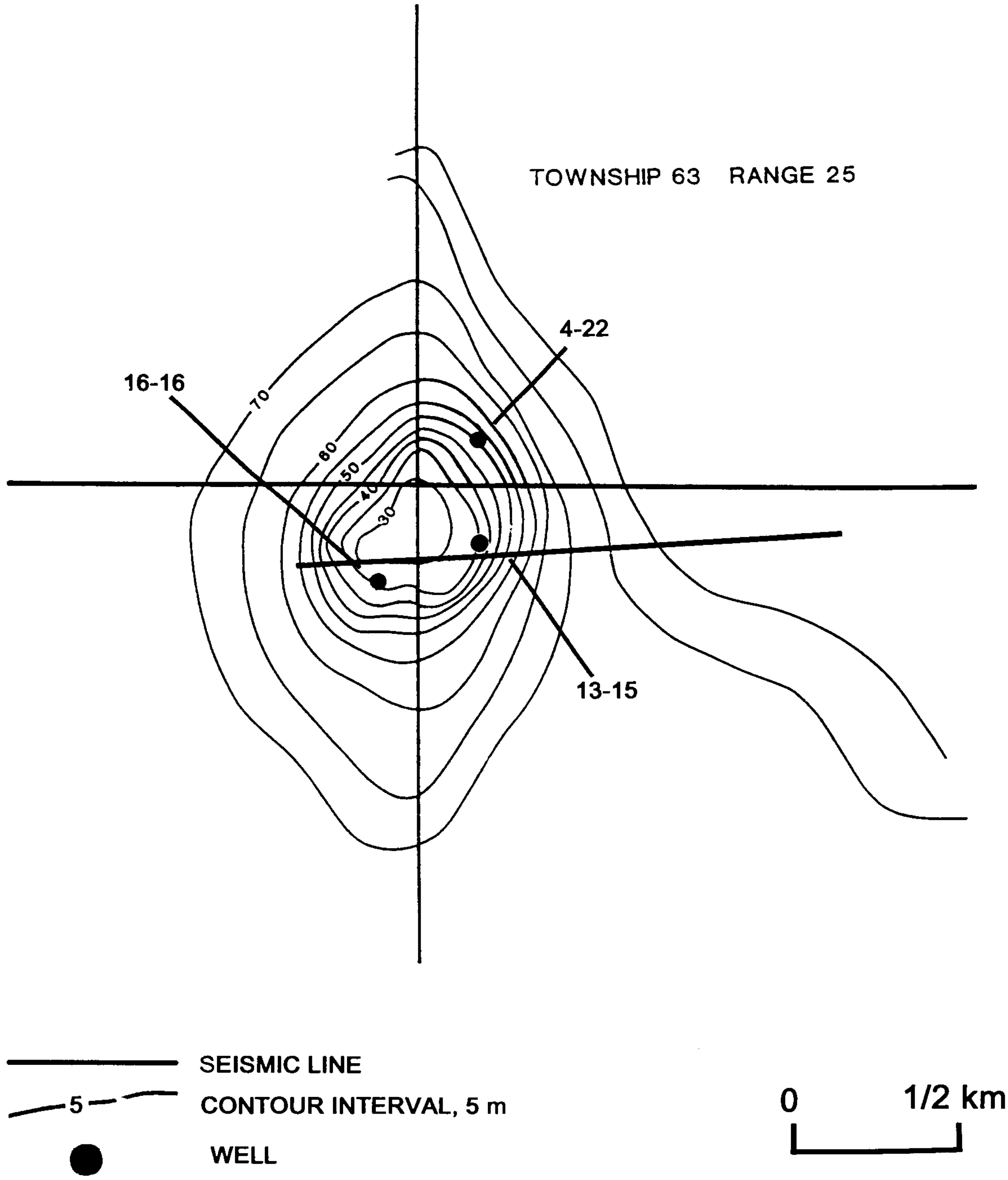

Figure 6.4 Ireton to Leduc isochron map resulting from the original interpretation of the seismic lines within the area of the low-relief reef. The oil pay-zone of the low-relief reef is interpreted to be as productive at the proposed well 13-15 as at the existing well 16-16 (from Hinds et al., 1993b, 1994c).

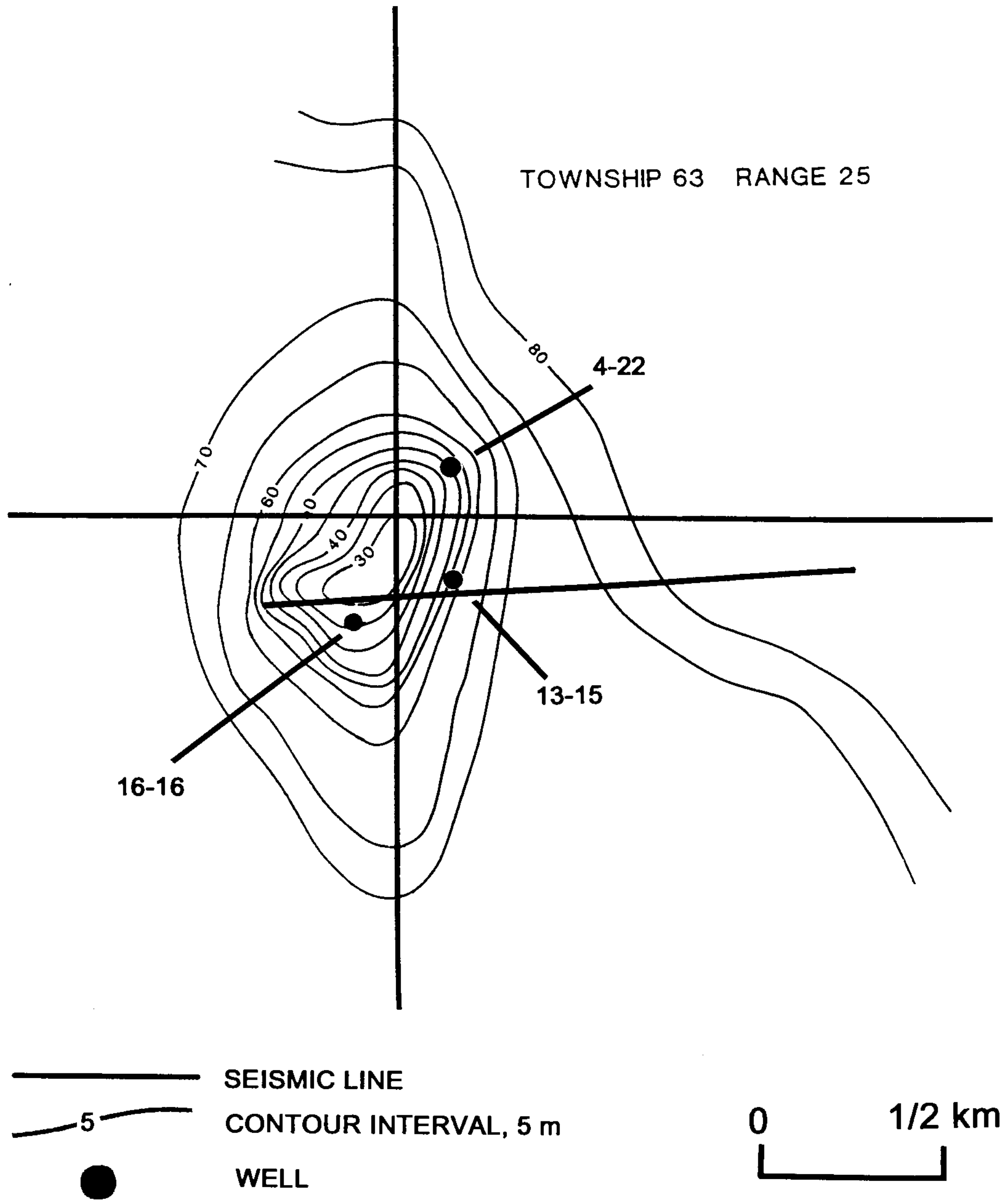

Figure 6.5 The preferred Ireton to Leduc isochron resulting from the updated interpretation (using the VSP results) of the seismic lines in the area of the low-relief reef, the VSP results and geologic borehole data. This interpretation shows the reef gradually rising out to 120 m from well 13-15 and then steeply rising towards well 16-16 (from Hinds et al., 1993b and 1994c).

The surface seismic line (normal polarity display; Fig. 6.3) is a stack of nominally 20-fold, split-spread, 120 prestack trace data, acquired using a patterned dynamite source (2 X 0.5 kg at 9 m depth; shotholes spaced 25 m apart) and DFS-5 recording equipment (8-128 hz filter). The seismometer groups consisted of nine, inline, 14 hz geophones spaced at 3.75 m. The geophone group and shot intervals were 25 and 75 m, respectively.

The seismic markers of principal interest correspond to the Mannville, Nordegg, Debolt/Belloy, Wabamun, Ireton, Z-marker (a regional marker within the inter-reef shales), and Leduc (Figs. 6.2 and 6.3). The Z-marker corresponds to the top of the Duvernay shales listed in the stratigraphic chart in Figure 6.2 and is caused by a change in the carbonate content within the Duvernay shale versus the overlying Ireton shale. The seismic image of the subsurface at well 13-15 (Fig. 6.3), was initially interpreted as comparable to that at the productive well 16-16 location; hence it was drilled. The high-amplitude event at about 1.9 s, at the 13-15 location, was mistakenly interpreted as the top of the reef. In retrospect, it is believed to be the off-reef Z-marker. Well 13-15 intersected the low-relief reef in a flank position below the oil/water contact (P. Pelletier, pers. comm.) and encountered 134 m of inter-reef shale (in comparison with 75 m of shale encountered in well 16-16). On the basis of the well results, it was suggested that the low-relief reef could rise abruptly to the west and that whipstocking in the direction of the productive 16-16 well should be considered.

The operators of well 16-16 were left with two alternatives: abandon the well or whipstock in the direction of well 16-16, bearing in mind that the further well 13-15 deviated from the original bottomhole location, the greater the Alberta Government imposed production penalty. In order to ascertain the cost-effectiveness of whipstocking the operators ran two VSP surveys: a near offset (252 m) and a far offset (524 m) VSP survey. It was on the basis of these data and the reinterpretation of the existing surface seismic, that the decision was made to abandon well 13-15 without any whipstock.

6.3 VSP acquisition

After an analysis of the 13-15 well geophysical logs and prior to abandonment, two VSP surveys were run at this well site in order to:

1) more accurately tie the surface seismic data and an interpretation thereof to the subsurface geology (in particular the top of the low-relief Leduc reef);

2) map the top of the reef over a distance of 150 m in the direction of the 16-16 well (with a view to whipstocking); and

3) differentiate primary reflections from both surface-generated and interbed multiples.

The near offset was chosen to be 252 m from well 13-15, the far offset to be 524 m; both are online with respect to the surface seismic line (Fig. 6.4). Two Vibroseis units were operated in series at each offset. The 12 s sweep ranged from 10 to 70 hz, the recording length was 15 s, and the cross-correlated output was 3 s. On average, six sweeps were summed for each geophone sonde location. MDS-10 recording instruments and a sampling interval of 1 ms were used. The recording filter was OUT/250; the instrument filter served as an anti-aliasing, lowpass filter with a ramp rolloff starting at 250 hz.

Well 13-15 extends 3620 m below the Kelly Bushing (at 878 m asl). Both source locations were at 868 m asl. The geophone sonde was lowered to the bottom of the well and raised at 20-30 m intervals. At each sonde location, the three component geophone tool was locked in place.

The two offsets were designed to be within the direction of the producing 16-16 well with the following interpretation considerations in mind:

1) if the slope of the reef was steep, a diagnostic seismic signature would be seen of the 252 m offset data; however a diagnostic shadow zone (null data) would be seen on the 524 m data;

2) if the crest was not steep but gradual, then both offset data would reflect the seismic image of the slope (the 252 m offset data would be a subset of the 524 m offset VSP data); and

3) if the slope was gradual but became steeper beyond the range of the near offset (252 m) VSP, then the 252 and 524 m offset data would both image the gradual slope but only the longer offset data would image the steeply sloped part of the reef.

6.4 Near offset (252 m) VSP interpretive processing

During the processing of the near offset VSP, a series of interpretive processing panels (IPPs) were designed (Hinds et al., 1993b and 1994c) to display the following :

1) separation of $\mathbf{Z_{up}(FRT)}$ and $\mathbf{Z_{down}(FRT)}$ data from the **Z(FRT)** data;

2) deconvolution of the $\mathbf{Z_{up}(FRT)}$ data to output the $\mathbf{Z_{up(decon)}(FRT)}$ using an inverse filter calculated from the $\mathbf{Z_{down}(FRT)}$ data; and

3) inside and outside corridor stacks (Hinds et al., 1989a) of both the $\mathbf{Z_{up}(+TT)}$ and $\mathbf{Z_{up(decon)}(+TT)}$ data.

6.4.1 P-wave separation

The separation of the upgoing and downgoing P-waves on the vertical (Z) geophone data is illustrated in the wavefield separation IPP (Hinds et al., 1989a) in Figure 6.6.

Panel 1 (Fig. 6.6) displays the normalized **Z(FRT)** data. In panel 2, high-amplitude surface-generated multiples, and less prominent interbed multiples can be seen in the **Z(-TT)** data. The surface-generated downgoing multiples can be recognized as continuous events arriving after the first break primary downgoing wavetrain on all of the traces, from the deepest to the shallowest receiver location (Hinds et al., 1989a). A downgoing multiple associated with

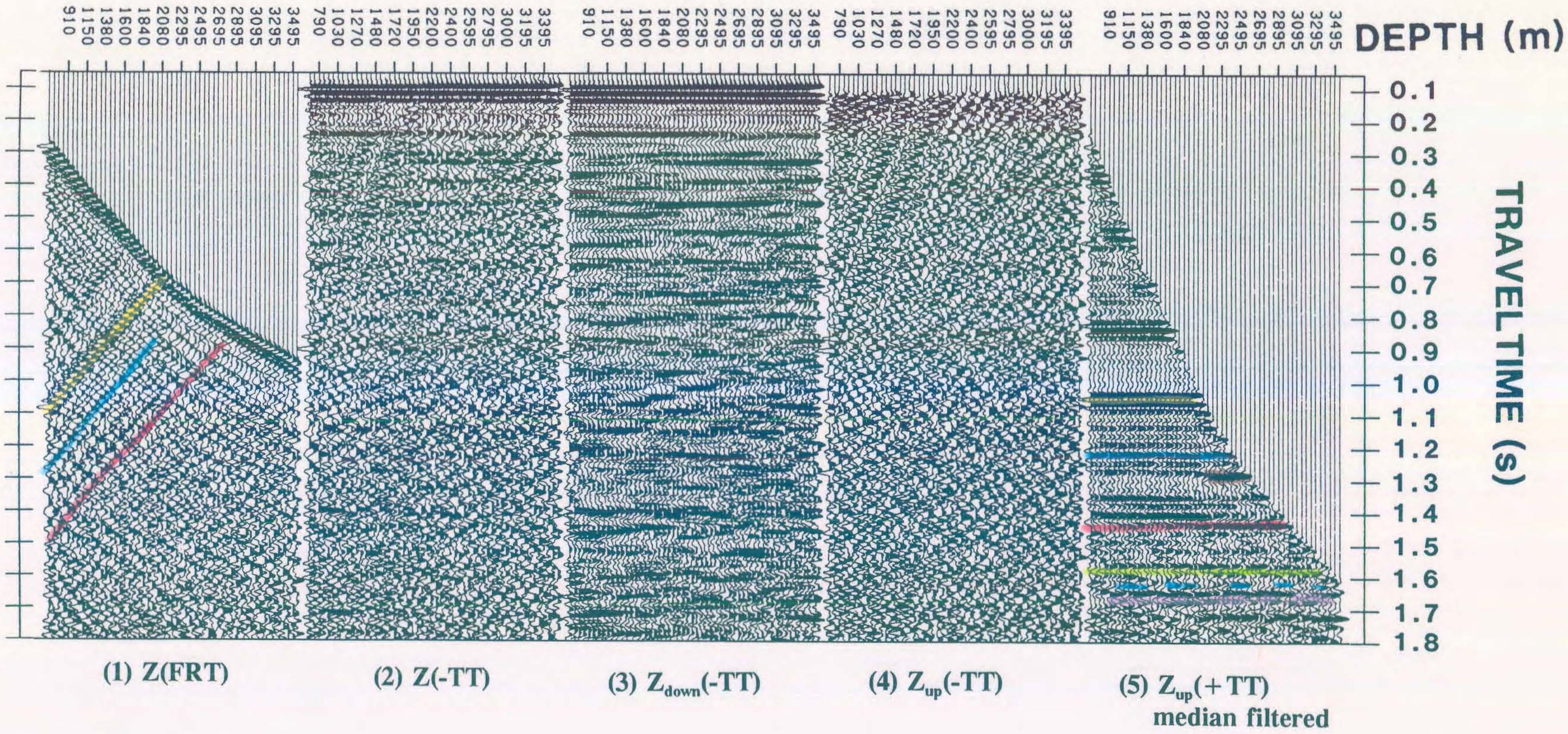

Figure 6.6 Interpretive processing panel depicting the wavefield separation of the near offset (252 m) offset Simonette VSP data (from Hinds et al., 1993b and 1994c).

the Mannville Formation interface is interpreted to start at the 2080 m trace (between 0.3 and 0.32 s; panel 2) and continue onto the deeper traces. The event may be an interbed multiple, since on panel 2, it does not appear to continue onto the shallower depth traces. The $\mathbf{Z_{down}}$**(-TT)** data in panel 3 do not assist in the interpretation since the median filter has smeared the event onto the shallower traces. An inspection of the $\mathbf{Z_{up}}$**(+TT)** data in panel 5 confirms that multiple interference is definitely originating from the Mannville Formation top interface.

The $\mathbf{Z_{down}}$**(-TT)** data were obtained from the **Z(-TT)** data using an eleven-point median filter and are displayed in panel 3. The residual $\mathbf{Z_{up}}$**(+TT)** data content in panel 3 are interpreted to be minimal since the data consist predominately of horizontally aligned downgoing events. The $\mathbf{Z_{up}}$**(-TT)** shown in panel 4 were separated from the **Z(-TT)** data by subtracting the $\mathbf{Z_{down}}$**(-TT)** as reviewed in chapter 2. The Mannville, Nordegg, Belloy/Debolt, Wabamun, Ireton, Z-marker and reefal Leduc events are interpreted in the median filtered $\mathbf{Z_{up}}$**(+TT)** data and shown in panel 5 of Figure 6.6.

6.4.2 Near offset VSP deconvolution

Multiple reflections are represented in the downgoing wavefield as shown in panel 3 of Figure 6.6. The initial downgoing pulse (except in the case of head wave contamination) is the primary downgoing P-wave; later downgoing arrivals are multiples. The deconvolution IPP was designed as shown in Figure 6.7 to enable the monitoring of the deconvolution process.

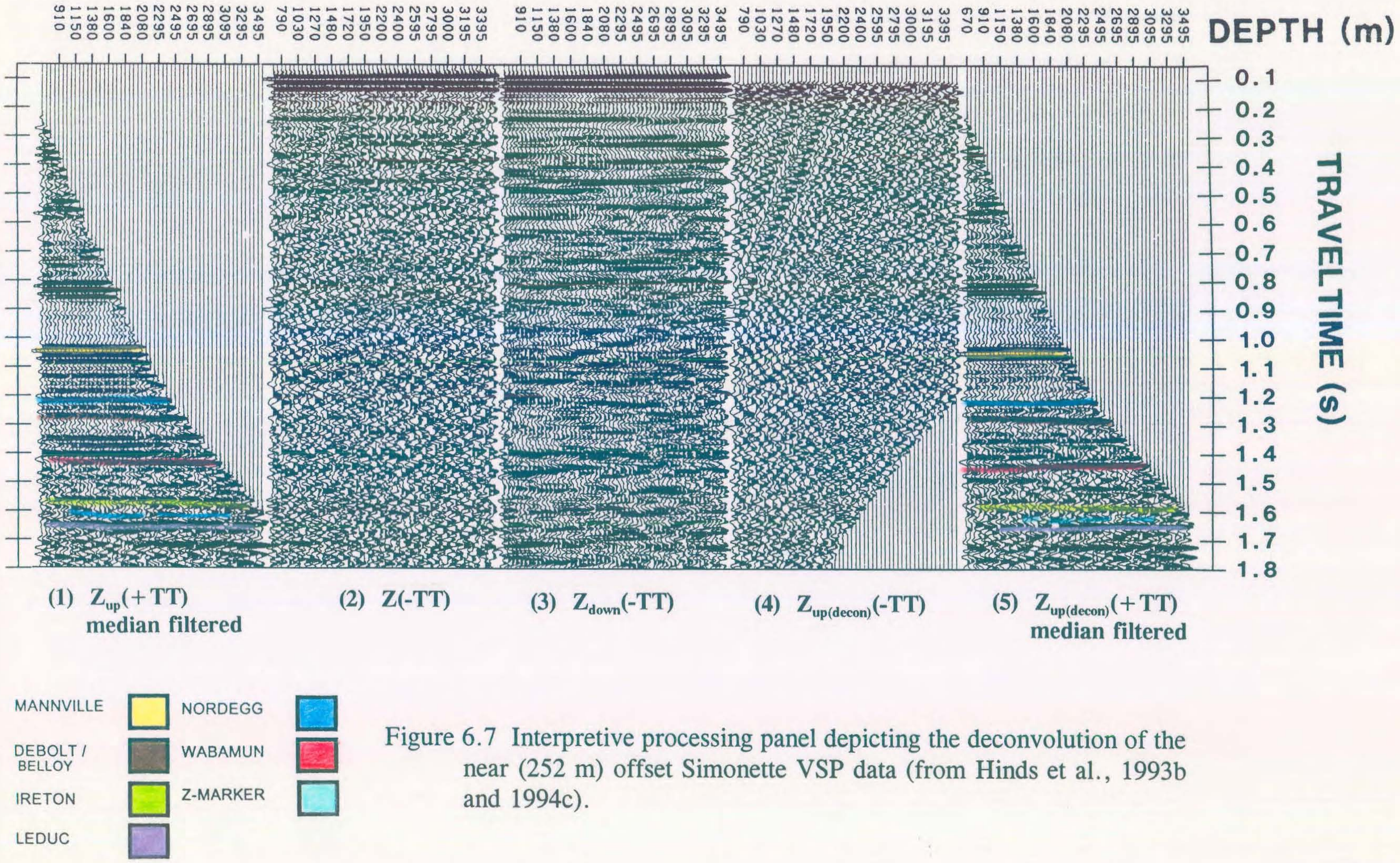

Figure 6.7 Interpretive processing panel depicting the deconvolution of the near (252 m) offset Simonette VSP data (from Hinds et al., 1993b and 1994c).

Panel 1 of Figure 6.7 is the median filtered $\mathbf{Z_{up}(+TT)}$ data. Panels 2, 3, and 4 are the $\mathbf{Z(-TT)}$, $\mathbf{Z_{down}(-TT)}$ and $\mathbf{Z_{up(decon)}(-TT)}$ data, respectively. The median filtered $\mathbf{Z_{up(decon)}(+TT)}$ data are displayed in panel 5.

A comparison of the $\mathbf{Z_{up}(+TT)}$ with $\mathbf{Z_{up(decon)}(+TT)}$ data, illustrates the effect of multiple contamination on the continuity of primary events. In panel 1 for example, the Debolt/Belloy event is high amplitude and continuous at sonde depths below the Mannville (from 2080 m to 2570 m). At shallower recording depths, the Debolt/Belloy event and a Mannville interbed multiple are interpreted to interfere. In more detail, the peak at 1.275 s on the left hand side of panel 1 is the interfering multiple. This event can be traced across the panel until the 2080 m trace. At that point, the Debolt/Belloy event peak (of lower frequency than the multiple) dominates and is continuous until the 2570 m trace; upon which it no longer exists since this is where the "first break" for that depth level now exists. On panel 5, deconvolution appears to have substantially reduced the effect of multiple interference as the Debolt event is much more continuous and the series of multiples immediately below the Mannville are strongly attenuated.

Within the zone from the Wabamun to Leduc Formation, multiple contamination is interpreted to be minimal since the events in this zone are continuous and unchanged after deconvolution. The Z-marker and Leduc events are continuous and do not exhibit either significant apparent time-structural relief or appreciable character variations. The description of the 524 m VSP interpretation will show that the far offset data do contain an interpreted multiple associated with the Wabamun interface in contrast to the near offset results presented above in which multiple generation at the Wabamun level is minimal.

6.4.3 Inside and outside corridor stacks

Multiple contamination on the $\mathbf{Z_{up}}$(+TT) data can be re-examined using the inside and outside corridor stacks of both the $\mathbf{Z_{up}}$(+TT) and $\mathbf{Z_{up(decon)}}$(+TT) data.

$\mathbf{Z_{up}}$(+TT) inside and outside corridor stacks along with the input data to the muting and stacking processes are shown in Figure 6.8. The amplitude of the Debolt/Belloy primary is weak on the $\mathbf{Z_{up}}$(+TT) inside corridor stack shown in panel 4 of Figure 6.8 in comparison to the same event on the outside corridor stack as displayed in panel 3. The Debolt/Belloy event at sonde depths shallower than 2080 m (above the Mannville) on the muted input data shown in panel 5 for the $\mathbf{Z_{up}}$(+TT) inside corridor stack is masked (destructively interfered with) by a possible interbed multiple. At depths greater than the Mannville (2080 m), the Debolt/Belloy event is unaffected by the multiple contamination, much higher in amplitude and 5-10 ms deeper in time therefore confirming that the bottom generating interface for this multiple is the Mannville Formation interface.

On the inside and outside $\mathbf{Z_{up(decon)}}$(+TT) corridor stacks shown in Figure 6.9, the upgoing multiples appear to have been substantially attenuated by deconvolution. As an example, the Mannville associated multiples that lie immediately beneath the Mannville primary event on the $\mathbf{Z_{up(decon)}}$(+TT) data are greatly attenuated with respect to the $\mathbf{Z_{up}}$(+TT) data. This can be seen by comparing panel 1 of Figure 6.8 to panel 1 of Figure 6.9 in the time window of 1.35 to 1.5 s. In Figure 6.8, the time window is contaminated with multiple reflection events (coloured turquoise blue in panels 1 and 4) whereas in Figure 6.9, the same time window is relatively free of multiples. One multiple reflection event to note lies just above

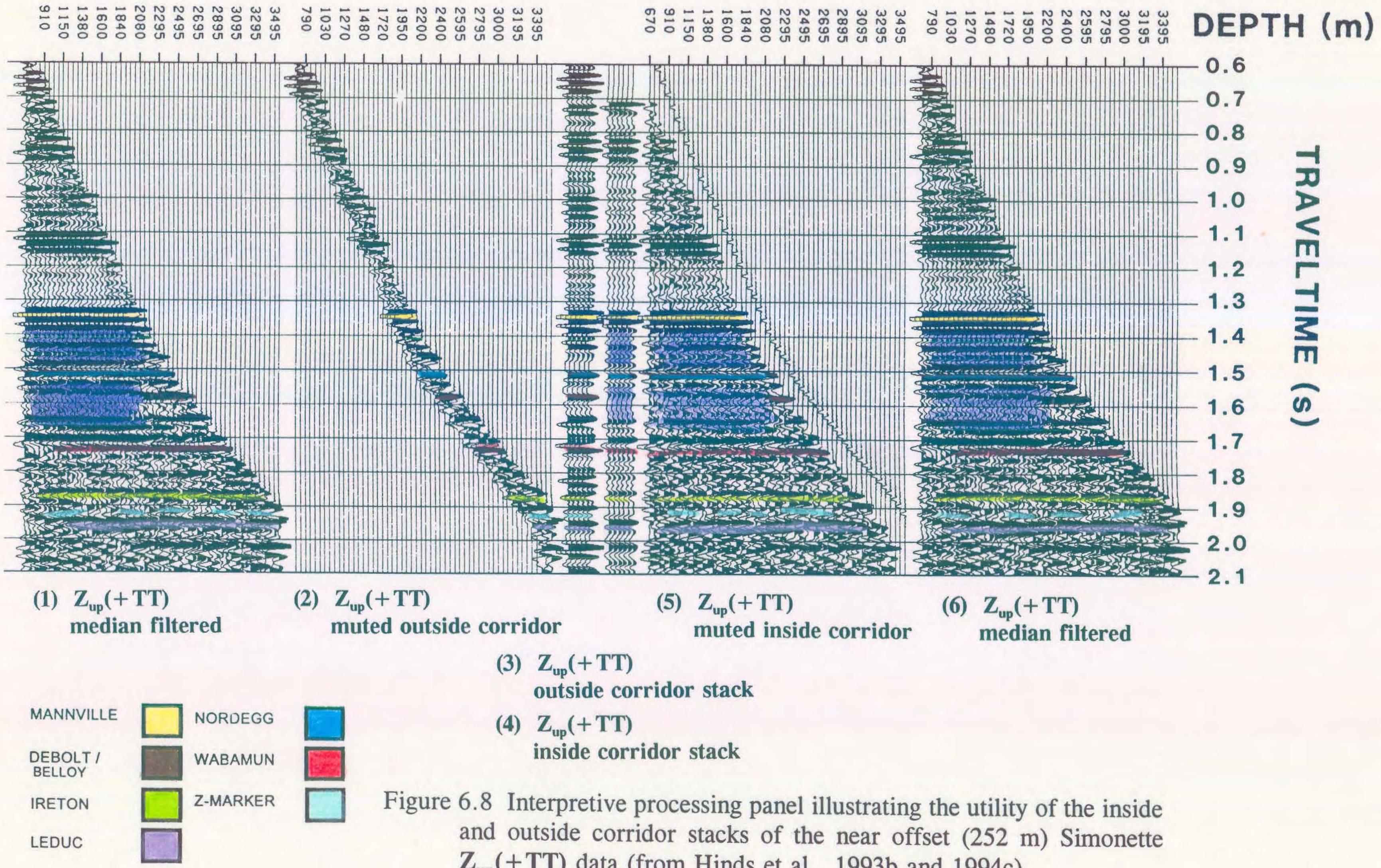

Figure 6.8 Interpretive processing panel illustrating the utility of the inside and outside corridor stacks of the near offset (252 m) Simonette Z_{up}(+TT) data (from Hinds et al., 1993b and 1994c).

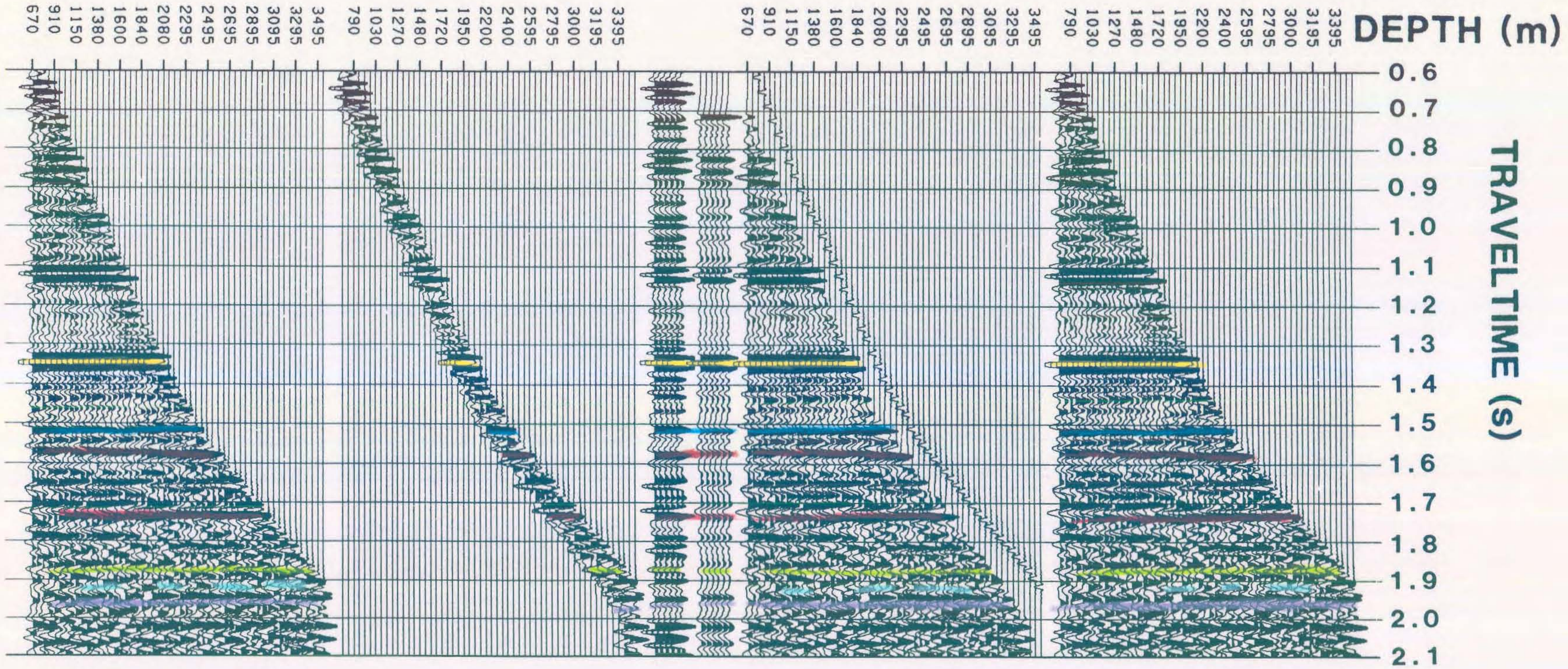

(1) $Z_{up(decon)}(+TT)$ median filtered

(2) $Z_{up(decon)}(+TT)$ muted outside corridor

(5) $Z_{up(decon)}(+TT)$ muted inside corridor

(6) $Z_{up(decon)}(+TT)$ median filtered

(3) $Z_{up(decon)}(+TT)$ outside corridor stack

(4) $Z_{up(decon)}(+TT)$ inside corridor stack

Figure 6.9 Interpretive processing panel illustrating the utility of the inside and outside corridor stacks of the near offset (252 m) Simonette $Z_{up(decon)}(+TT)$ data (from Hinds et al., 1993b and 1994c).

the Nordegg primary event at 1.48 s. On panel 1 of Figure 6.8, the event is dominant; however in panel 1 of Figure 6.9 (after deconvolution), the event is attenuated.

Some primary events recorded between the Mannville and Nordegg primary reflection events can only be seen on the few traces beyond the deepest trace recording the Mannville primary event. These few peaks will be included in the outside corridor stack. One such event is at 1.45 s which is preserved across the entire depth range of 670 to 2295 m once deconvolution is done. Since the depth interval between these primary events generated between the Mannville and Nordegg interfaces represents only a few traces, it causes the use of corridor stacks alone difficult to interpret without including the unmuted and muted corridor stack data on the same IPP (Hinds et al., 1989a).

6.5 Interpretive processing of the far offset VSP data

During the production consulting in 1987, the triaxial processing was not performed whilst the rig was on standby. The VSP-CDP mapped data recorded in 1987 used the $\mathbf{Z_{up}(+TT)}$ from the 524 m offset without the assistance of polarization analysis. The processing (Hinds et al., 1993b and 1994c) presented in this chapter is more extensive. The **Z(FRT)**, **X(FRT)** and **Y(FRT)** data contain nonpartitioned elements of the up- and downgoing P- and SV-wavefields. Hodogram-based rotation and time variant polarization rotation IPP's used in the processing of the far offset for the Simonette 524 m offset data (Hinds et al., 1989a; Hinds et al., 1991b; Hinds et al., 1993b and 1994c) are presented below to reveal that wavefield partitioning has significant implications for the interpretation.

6.5.1 Hodogram based rotation

The **Z(FRT)**, **X(FRT)**, and **Y(FRT)** data are presented in Figure 6.10 as panels 1, 2, and 3, respectively. The hodogram-based method initially polarized the components of the **X(FRT)** and **Y(FRT)** data outputting the **HMIN(FRT)** and **HMAX(FRT)** data (Hinds et al., 1989a; Hinds et al., 1993b and 1994c) shown in panels 4 and 5, respectively. **HMAX(FRT)** data display consistent primary downgoing P-wave first breaks indicating that the first set of rotations was relatively successful. The **HMAX(FRT)** data also contains mode-converted SV events (colored purple) that originate in the region of the Mannville reflector.

The **Z(FRT)** and **HMAX(FRT)** data were input to the second rotation which polarized the downgoing P-waves. Since the source offset distance is 524 m and the depth of the well is 3270 m, the **HMAX'** and **Z'** polarization axis were near vertical and horizontal, respectively. The resultant **Z'(FRT)** and **HMAX'(FRT)** data are shown in panels 6 and 7, respectively. The downgoing P-wave events are resident on the **HMAX'(FRT)** data; however, both the **HMAX'(FRT)** and **Z'(FRT)** data contain upgoing P-wave events. This indicates that the data will need to undergo time-variant polarization to separate the upgoing P-wave events onto a single data panel ($\mathbf{Z''_{up}}$) before interpretation.

The **Z'(FRT)** data (panel 6) contains the mode-converted downgoing shear wave primaries and possible multiples. In more detail, the first break on the 2080 m trace (representing the depth of the Mannville) can be approximated to be at 0.68 s on panel 6. At that point, the mode-converted downgoing SV event with a greater slope than the downgoing P-wave (the shallowest event coloured purple) can be traced down to 1.12 s on the 3570 m trace. Two

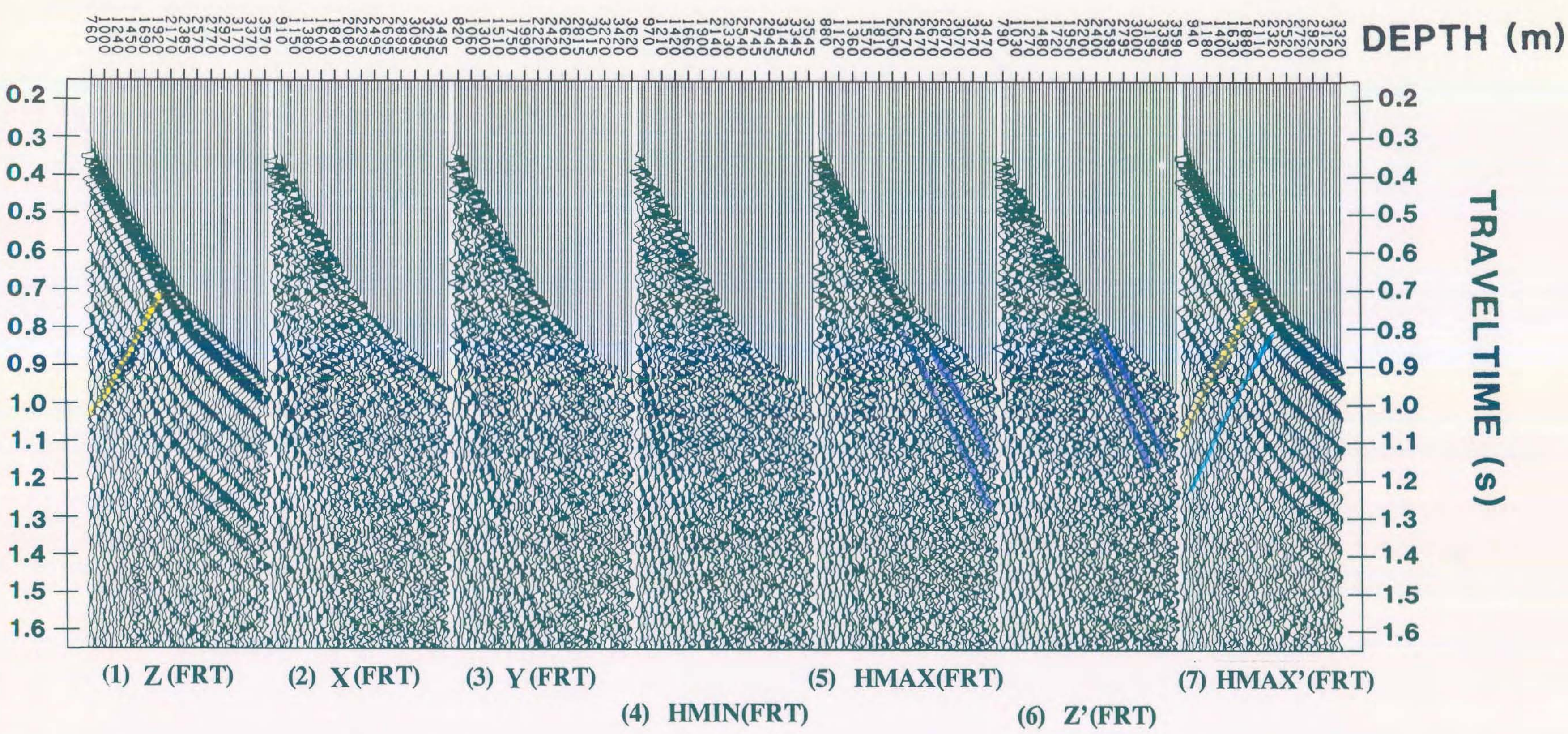

Figure 6.10 Interpretive processing panel depicting the hodogram-based rotation of the far offset (524 m) Simonette VSP data (from Hinds et al., 1993b and 1994c).

visible, downgoing SV-multiples (also coloured purple but arriving later in time than the primary downgoing SV primary event) parallel the primary and arrive within a 150 ms window on the 3570 m trace.

6.5.2 Time-variant model-based rotation

In the first stage of the time-variant model-based rotation, **Z'(FRT)** and **HMAX'(FRT)** data were wavefield separated (using F-K filtering; see chapter 2 for examples) into **$HMAX'_{down}$(FRT)**, **$HMAX'_{up}$(FRT)**, **Z'_{down}(FRT)** and **Z'_{up}(FRT)** data. The **$HMAX'_{down}$(FRT)** is retained and used in the deconvolution of the **Z''_{up}(FRT)** data in the following section. The deconvolution of the polarized far offset VSP data was not done during the 1987 processing and interpretation clarity will result from the deconvolution results shown below.

The **$HMAX'_{up}$(FRT)** and **Z'_{up}(FRT)** data shown as panels 1 and 2 in Fig. 6.11, respectively, were derotated (Hinds et al., 1989a) to output the **$HMAX_{up(derot)}$(FRT)** and **$Z_{up(derot)}$(FRT)** data shown in panels 3 and 4, respectively. Most of the upgoing P wave events have been distributed back onto the Z-type axis, **$Z_{up(derot)}$(FRT)**. In the **Z(FRT)** data shown in panel 1 of Fig. 6.10, the dominant downgoing P-waves were much higher in amplitude than the upgoing events resulting in the upgoing events being difficult to interpret. Following the wavefield separation, the separated upgoing P wave events in the **$Z_{up(derot)}$(FRT)** data are easily traceable within the data.

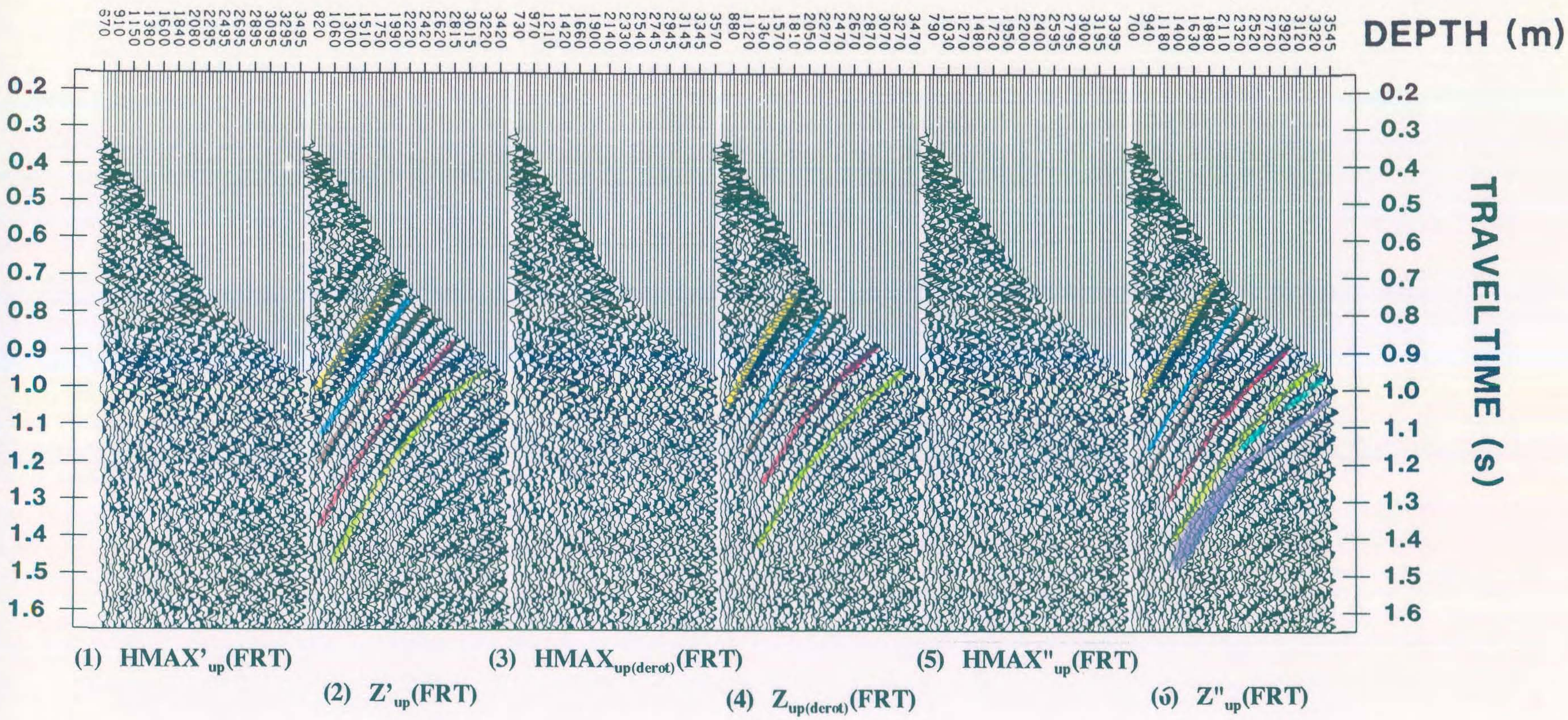

Figure 6.11 Interpretive processing panel depicting the time-variant model-based rotation of the far offset (524 m) Simonette VSP data (from Hinds et al., 1993b and 1994c).

The upgoing P-wave events on the $\mathbf{Z_{up(derot)}(FRT)}$ data shown in panel 4 are improperly aligned, particularly those generated by shallow reflectors, because of the choice of using a single rotation angle per data trace. These data have been derotated but the upgoing P-wave events are still partitioned on both output data sets, $\mathbf{Z_{up(derot)}(FRT)}$ and $\mathbf{HMAX_{up(derot)}(FRT)}$, due to the non-zero source offset.

To correct for misalignment, time-variant rotation angles were calculated (Hinds et al., 1991b; Hinds et al., 1993b and 1994c) and applied to every pair of traces in panels 3 and 4. The resultant $\mathbf{HMAX''_{up}(FRT)}$ data (panel 5) contains the residual downgoing SV-wave data left over in the data following wavefield separation. The $\mathbf{Z''_{up}(FRT)}$ data predominantly contains the upgoing P-wave events. On the $\mathbf{Z''_{up}(FRT)}$ data, shallow events (originating at 0.58 s between the traces for 1630 to 1750 m) are better isolated (onto a single panel) than on either the $\mathbf{Z_{up(derot)}(FRT)}$ data or $\mathbf{HMAX'_{up}(FRT)}$ data panels.

6.5.3 VSP-CDP mapping of the far offset VSP data

A VSP-CDP and migration IPP for the far offset $\mathbf{Z''_{up}(+TT)}$ and $\mathbf{Z''_{up(decon)}(+TT)}$ was designed to facilitate the interpretation of the interfering multiples and subsurface structure (Hinds et al., 1991b; Hinds et al., 1993b and 1994c). The $\mathbf{Z''_{up}(+TT)}$ data shown in Figure 6.12 were used for the interpretation of the low-relief Leduc reef. The appearance of many anomalous events arising from multiple contamination on the $\mathbf{Z''_{up}(+TT)}$ data (such as the event at 1.8 s) makes the interpretation of this plot along with the VSP-CDP (panel 3) and Kirchhoff migrated $\mathbf{Z''_{up}(+TT)}$ data difficult.

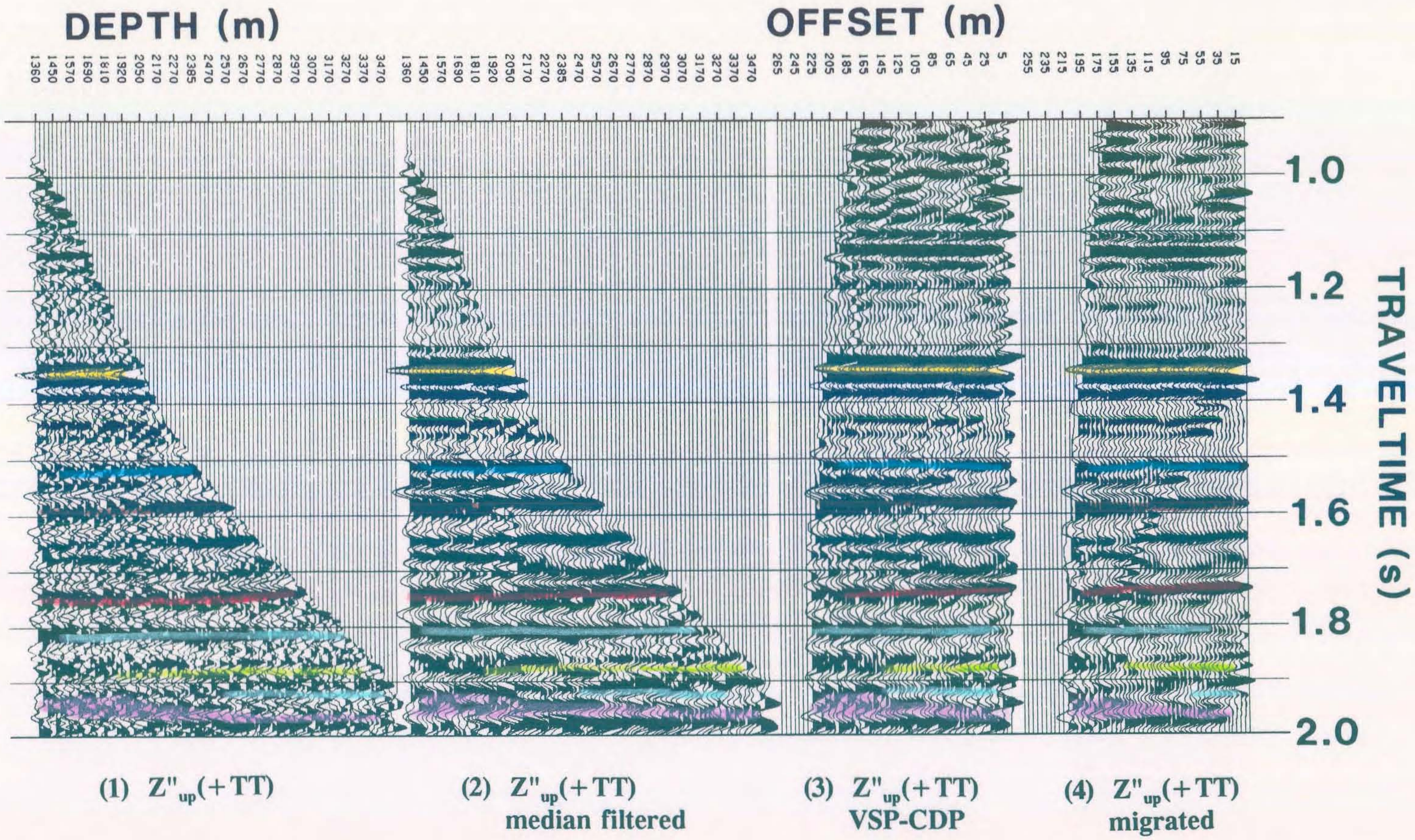

Figure 6.12 Interpretive processing panel showing the VSP-CDP transformed and Kirchhoff migrated far offset (524 m) $Z''_{up}(+TT)$ data (from Hinds et al., 1993b and 1994c).

The interpretation of the Leduc reef event is that the reef slope rises at 145 m away from the well; however the multiple events may be influencing the interpretation through destructive and constructive interference at the Leduc level.

Because of the relatively small offset of the source (524 m) in comparison to the overall depth of the borehole, far offset VSP deconvolution was attempted on the $\mathbf{Z''_{up}(+TT)}$ data as was shown in chapter 2. Nonmedian filtered $\mathbf{Z''_{up(decon)}(+TT)}$, median filtered $\mathbf{Z''_{up(decon)}(+TT)}$, VSP-CDP mapped (Dillon and Thomson, 1984) $\mathbf{Z''_{up(decon)}(+TT)}$ and Kirchhoff migrated $\mathbf{Z''_{up(decon)}(+TT)}$ data are shown, respectively, in panels 1-4 of Figure 6.13.

Two different sets of upgoing P-wave multiples are prevalent in Figure 6.12. One set of multiples are associated with the Mannville event. The nondeconvolved VSP-CDP and migrated data (Fig. 6.12) show Mannville (possibly interbed) multiples interfering with deeper P-wave primaries between 1.4 and 1.7 s. (specifically, 1.43, 1.56 and 1.68 s). Significant multiple contamination is interpreted between the shallowest trace and the 2080 m trace (top Mannville). Three multiple reflections are evident (coloured purple); the first Mannville multiple can be seen at 1.45 s, the second at 1.56 s (in between the Nordegg and Debolt primaries) and the third at 1.68 s.

The second set of multiples proved to be the most troublesome with respect to the reef interpretation during the initial processing done in 1987. There is a strong event (coloured light blue) below the Wabamun in the $\mathbf{Z''_{up}(+TT)}$ data at 1.8 s. It exists on the shallow traces down to the Wabamun and then abruptly disappears on the deeper traces from the

Wabamun reflector to total depth of the borehole. Was the interpretation of the reef events affected by this multiple event if the next occurrence of this Wabamun multiple existed? The interpreted reef flank shown in Figure 6.12 begins to rise around 145 m away from the borehole at 1.95 s up to 1.92 s. On the depth and time plots, the rise does not corresponds with the truncation of the multiple seen above at 1.8 s. This gives confidence in the interpretation that the rise in the reef event is due to the imaging of the reef slope; however interpretive processing must be used when faced with this decision!

In Figure 6.13, deconvolution has severely attenuated the Mannville and Wabamun multiple. The Mannville associated multiple events at 1.45, 1.56 and 1.68 s are attenuated and the Wabamun associated multiple event at 1.8 s is reduced from a dominant event to low amplitudes remnants. The Mannville, Nordegg, Debolt/Belloy, Wabamun, Ireton, Z-marker and Leduc events can now be more confidently correlated. The Leduc event can be interpreted on both the VSP-CDP and Kirchhoff migrated displays of Figure 6.13 to verify the interpretation of the nondeconvolved VSP-CDP and migrated data in the panels of Figure 6.12. The Z-marker (Fig. 6.13) rises gradually away from the location of the 13-15 well. The Leduc, although less discernable, is interpreted to rise gradually away from the borehole (basal Leduc) and rise to reef top at about 120-145 m from the borehole. The reflection from the top of the reef visually merges with the Z-marker event.

These results were used to assist in the construction of the preferred Ireton to Leduc isochron map shown earlier in Figure 6.5 (Hinds et al., 1991b and Hinds et al., 1993b and 1994c).

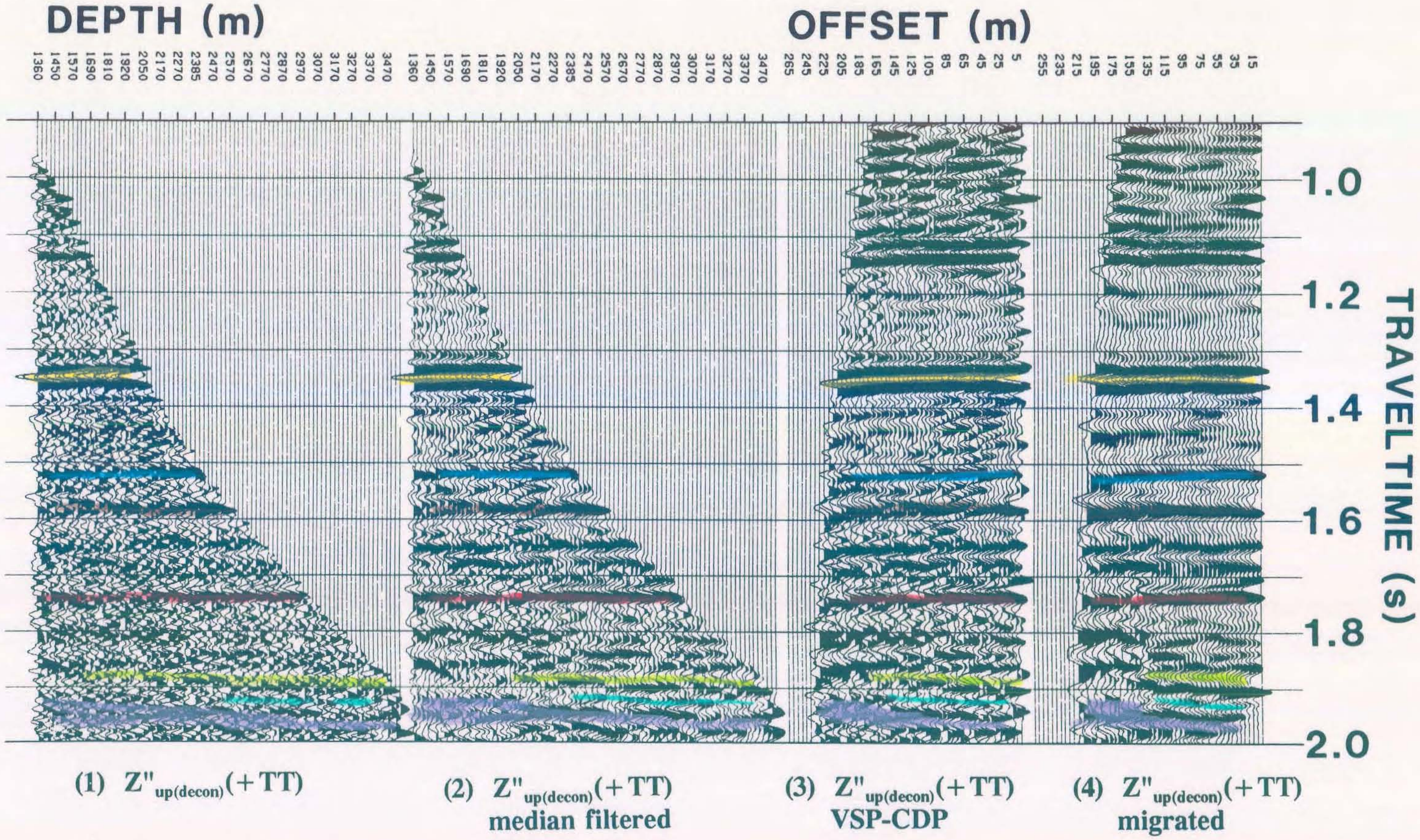

Figure 6.13 Interpretive processing panel showing the VSP-CDP transformed and Kirchhoff migrated far offset (524 m) $Z''_{up(decon)}(+TT)$ data (from Hinds et al., 1993b and 1994c).

6.6 Integrated interpretive display

On the left-hand side of the integrated interpretive display shown in Figure 6.14, sonic logs for wells 16-16 and 13-15, nondeconvolved, near offset, inside and outside corridor stacks are time-tied to the post-VSP interpretation of the surface seismic data. On the right-hand side, the $\mathbf{Z''_{up(decon)}(+TT)}$ data is time-tied to both the well 13-15 sonic log, and the deconvolved, near offset outside corridor stack. The horizontal (depth axis) of the $\mathbf{Z''_{up(decon)}(+TT)}$ data corresponds to the same scale used for the well 13-15 sonic and gamma ray log depth display.

The correlated data shown in Figure 6.14 allow for the confident interpretation of the surface seismic line and the identification of the Mannville, Nordegg, Debolt/Belloy, Wabamun, Ireton, Z-marker, and Leduc events. The Leduc event can be tied exactly at well 16-16 using the integrated sonic log from that well. The sloping reef event from well 16-16 to well 13-15 can be interpreted through the trough that gently slopes deeper in traveltime. Note that within the inter-reef shale interval, the sonic-log based synthetic seismogram is a poor fit to the VSP and surface seismic for the Ireton, Z-marker and Leduc events exhibiting up to a 5 ms tie. The sonic measurements could be at fault in that wellbore effects such as washouts, or the increased concentration of heavy drilling fluids injected into the borehole (intended to prevent a blowout) could have changed the sonic character of strata in the vicinity of the wellbore. Since the well was left open during the interpretation of the VSP survey data, it is reasonable to assume that the well engineers took precautionary steps to stabilize the fluids within the well. Alternatively, these misties could be related to wavelet variability or phase problems with the data (Hinds et al., 1993b). Whatever the source, such

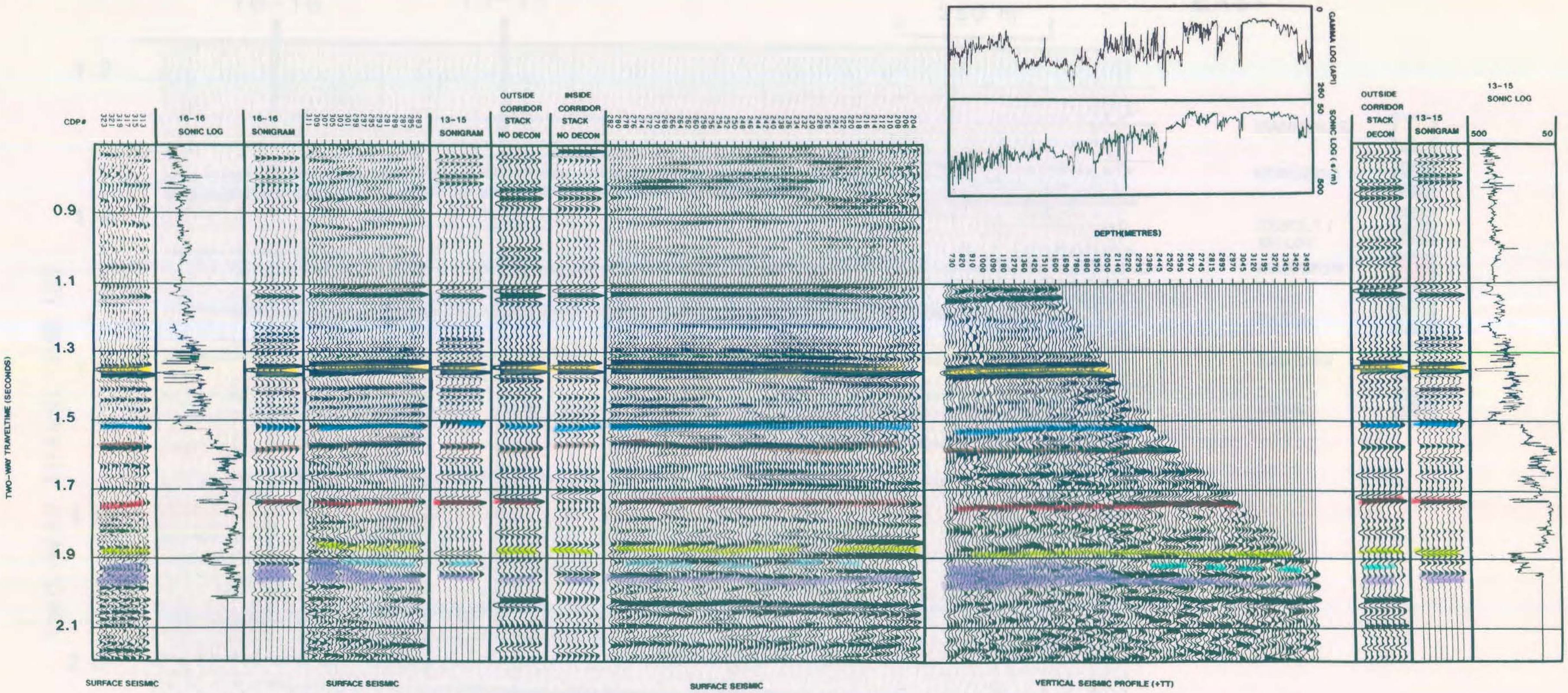

Figure 6.14 Integrated interpretive display showing the interpretation of the available exploration data for the Simonette reef case study (from Hinds et al., 1993b and 1994c).

discrepancies between sonic-log based synthetic seismograms and seismic data provide additional justification for acquiring seismic profile data.

The preferred version of the surface seismic section (shown as a normal polarity display in Fig. 6.15) differs slightly in several respects from the pre-well interpretation (Fig. 6.3). Of particular significance is that on the updated version, the Z-marker is present at the well 13-15 location, indicating that the well is situated in a flank position. The reinterpretation of the seismic line exhibits a flat reef extending from the borehole out to 100-120 m from the borehole. This is in agreement with the interpreted near and far offset VSP data. Beyond the coverage of the VSP, the reef crests. With respect to lateral variations in the thickness of the inter-reef shale isochron values (shale thinning is indicative of reefal thickening) the following interpretations can be made:

1) the inter-reef shale isopach as derived from the VSP data is 136 m (isochron value of 63 ms) on the trace nearest the 13-15 well;
2) the shale is 120 m (55 ms) at distances on the order of 100 m laterally from the well; and
3) the shale is 102 m (47 ms) at traces representing a distance of around 150 m from the well.

On the basis of the reinterpreted surface seismic and VSP data, a revised inter-reef shale isochron map (incorporating available well and surface seismic data) was drafted (Fig. 6.5). The 13-15 exploratory well is shown to be in a reef flank position, and indicates that the crest of the low-relief reef is in excess of 150 m west of well 13-15.

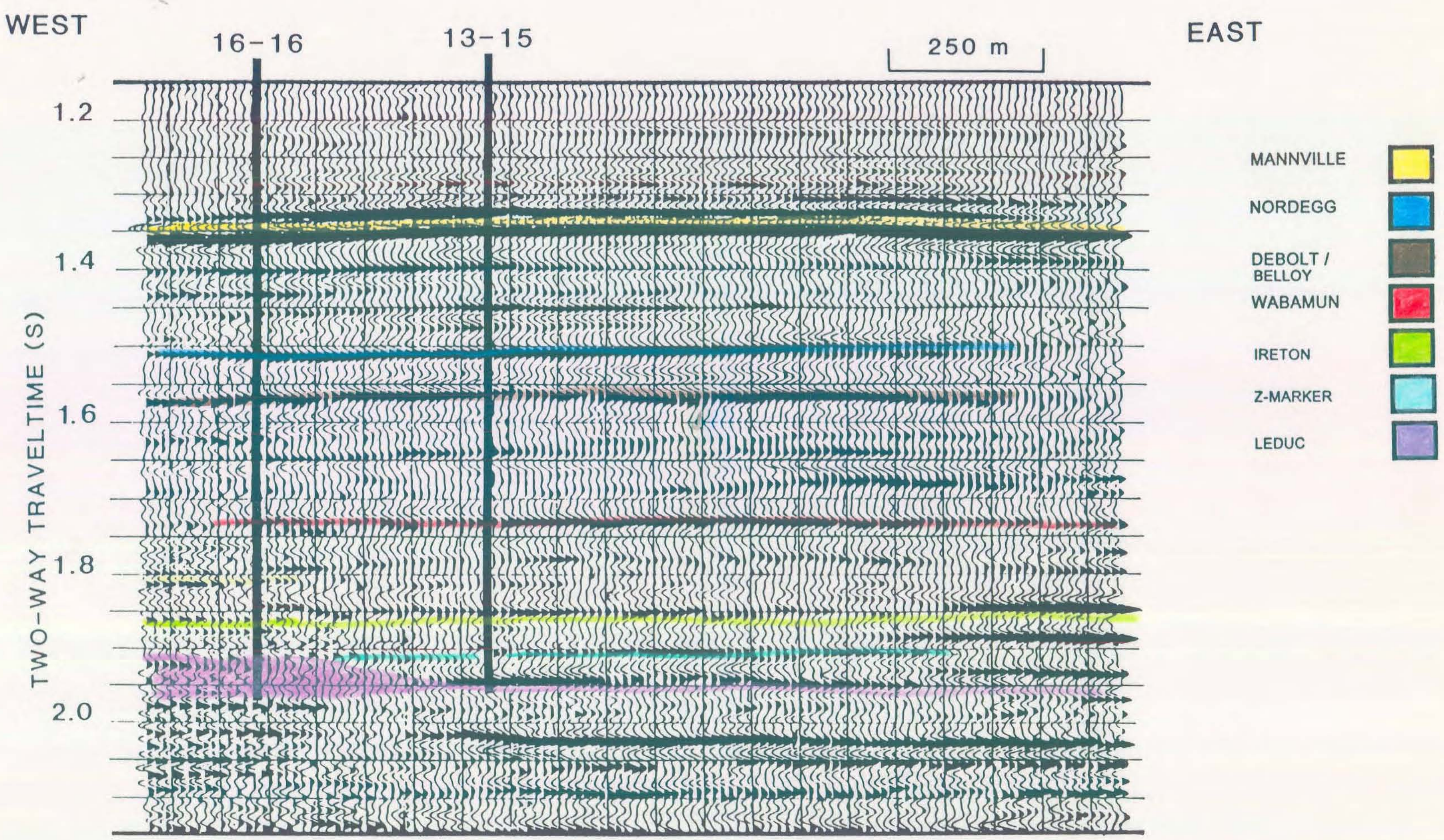

Figure 6.15. Current, preferred interpretation of the example seismic section. The Z-marker is laterally continuous at the 13-15 well location and the reef slope has been reinterpreted to be at least 150 m to the East of well 13-15 (from Hinds et al., 1993b and 1994c).

6.7 Conclusions

The 13-15-63-25 W5M exploratory well was drilled into low-relief Leduc reef in the Simonette area, Alberta. The well was prognosed to intersect the crest of the reef and to encounter about 50-60 m of pay. Unfortunately, according to the interpretation of all of the well data, it appears that the well was drilled into a flank position and ultimately abandoned. The decision to abandon the well, as opposed to whipstocking, was made after the acquisition and interpretive processing of the near and far offset VSP data, and after the reanalysis of existing surface seismic data. The VSP data were acquired and interpreted while the drill rig remained on-site, awaiting the decision to whipstock or abandon.

On the basis of VSP data the operator was able to: (1) determine an accurate tie between the surface seismic data (Fig. 6.15) and the subsurface geology, and identify a mistie between the surface seismic and sonic log seismogram; (2) determine that the reef was not close enough to well 13-15 to make whipstocking a viable option given the production penalties involved in drilling out of the target area; and (3) identify surface-generated and interbed multiples, and ascertain their effect on the surface seismic.

CHAPTER 7

SUMMARY AND CONCLUSIONS

The first two aims of this study were to:

(1) develop the methodology of Interpretive Processing (Hinds et al., 1989a) for VSP data using the interpretive processing panels (IPP), interactive data processing, integrated log display (ILD), integrated seismic display (ISD) and the integrated interpretation display (IID); and

(2) review the usage of the processing steps in the individual IPP to illustrate the incorporation of VSP interpretation to minimize processing artifacts (Hinds et al., 1994c).

A suggested processing runstream that was initially used in the VSP interpretive processing work of Hinds et al (1989a) was used as a starting point in the development of the interpretive processing displays. The major factors within VSP processing such as wavefield separation, near offset deconvolution, far offset data hodogram-based and time variant polarization, VSP-CDP transformation and migration were thoroughly discussed and used to illustrate the use of interpretive processing to locate, understand and correct for processing artifacts within the data processing sequences.

The interpretive processing panels were used to quality control processing routes (such as wavefield separation shown in Flowcharts 1 through 6), link seismic data to geologic well log data (as in the ILD), merge VSP-CDP transform (or migration) results with surface seismic (as in the ISD) and to collect and merge all available exploration data into a single descriptive display (as in the IID). For the wavefield separation, the median filter (plus subtraction), K-L, F-K and τ-P based method were described with the emphasis being on the interpretation of possible processing artifacts inherent in the use of each method and their resolve. In the F-K based wavefield separation, batch processing and interactive F-K filtering were highlighted and the use of each was described through example data processing. Several different ways to use the same method to attack a particular "noise" problem such as multiple or tubewave contamination was shown for the F-K and τ-P based methods.

Multiple contamination and attenuation for both near and far offset data were shown through the use of the deconvolution IPP, inside and outside corridor stack IPP and the far offset deconvolution IPP. The final interpretation of the lateral extent of anomalies were shown thorough the use of the IPP's that included the VSP-CDP (migration) results. The concluding exploration picture was summarized through the use of the IID. In all of these displays for the various processing procedures, integrated geophysical/geological interpretation quality controlled and guided corrective or further processing.

The third and fourth aims were to:

(3) present the usage of VSP interpretive processing in four case studies, Lanaway Field (Hinds et al., 1989a; Hinds and Botha, 1989b; Hinds et al., 1994a and 1994c);

Ricinus Field (Hinds at al., 1989a; Hinds and Botha, 1989c; Hinds et al., 1993c; Hinds et al., 1994c), Fort. St. John Graben (Hinds et al., 1991a, Hinds et al., 1993a; Hinds et al., 1994b; Richards et al., 1994; Hinds et al., 1994c) and Simonette Field (Hinds et al., 1991b; Hinds et al., 1993b and 1994c); and

(4) further the method of integrated geophysical/geological interpretation (Anderson, 1986) using the case studies.

In the Lanaway Field case study shown in Chapter 3 which deals with oil and gas exploration along the Rimbey-Leduc-Meadowbrook carbonate reef "chain" in Alberta, Canada, the original interpretation of the seismic data which indicated 80 m of possible anomalous accretionary reef growth led to the drilling of a well that penetrated oil and gas bearing reef that was similar to surrounding successful Leduc wells. By means of interpretive processing through the use of IPP's and IID, an updated interpretation was developed that was consistent with the geological log data. Multiple contamination was examined and three possible explanations for the anomalous seismic character and time-structural anomaly was stated. Of these three explanations, the presence of possible Winterburn patch reefing and the tuning effect on the seismic data caused by surrounding Ireton drape was put forth as most likely to be the cause of the seismic anomaly (Hinds et al., 1989a; Hinds and Botha, 1989b; Hinds et al., 1994a and 1994c). The final interpretation differed from the original as the correct seismic placement of the Leduc reef at the well location was found.

In the Ricinus Field case study shown in Chapter 4 which deals with gas exploration in the Ricinus Leduc carbonate atoll reef in central Alberta, the original interpretation of the seismic data which predicted the intersection of Leduc reef led to the drilling of a well that penetrated off-reef Woodbend Group shales. A near and far offset VSP surveys were run. Through the use of interpretive processing using near and far offset IPPs and ISD, the seismic was correlated to the geological logs. An updated geological model was developed and the final interpretation differed from the initial interpretation as the edge of the reef (in the direction of the far offset source location) on the seismic section was postulated to at least 500 m away from the well.

In the Fort St. John Graben case study shown in Chapter 5 which deals with channel sand gas accumulations in Lower Carboniferous strata, the original interpretation predicted the intersection of gas bearing basal Kiskatinaw sandstones and the presence of a single fault between the VSP well and well 2-25 to the North. The interpretation led to the drilling of a basal Kiskatinaw sandstone with a high shale content which was non-commercial. A near offset and two far offset VSP surveys were run. The interpretive processing of the near offset VSP data led to an updated seismic correlation to the geology at the well in addition to the revealing of extensive multiple contamination. The interpretive processing of the far offset VSP data (FSJG1) which imaged the subsurface towards the seismic line (and the VSP well) led to the interpretation of a lateral character anomaly within the basal Kiskatinaw event (which could be caused by increased shale content) and the location of two faults throughout lower and upper Carboniferous strata which were unresolved on the surface seismic (Hinds et al., 1993a and 1994b; Hinds et al., 1994c). The far offset VSP data (FSJG2) which imaged the subsurface to the East of the well (away from the seismic line and the VSP well) explored for basal Kiskatinaw channel sands and faulting. The interpretive processing showed a continuous basal Kiskatinaw and the imaging of two faults which are interpreted to be related to the faulting seen on the other far offset VSP data. The updated interpretation differed from the original due to the accurate mapping of the lower and upper Kiskatinaw (which produced gas at the VSP well) in the vicinity of the VSP well and the detailing of faulting which was poorly imaged by the surface seismic.

In the Simonette Field case study shown in Chapter 6 which deals with oil exploration in the Simonette Reef in North-western Alberta, the original interpretation of the seismic data which prognosed the penetration of 50-60 m of productive carbonate reef led to the drilling of a well that penetrated off-reef shales. A near and far offset VSP were run whilst the drilling rig was on-site in order to determine if whipstocking the well towards a known producing well 16-16 (within the same reef) was viable. The interpretive processing of the near offset data determined an accurate correlation to the geological wells, identified possible multiple contamination and showed that the edge of the reef was not evident up to distance of 120 m from the VSP well. The interpretive processing of the far offset data showed possible Wabamun multiple contamination, confirmed the reef slope interpretation from the near offset VSP data, located the edge of the reef to be approximately 155 m from the VSP well and showed that the reef did not reach the buildup that was found in well 16-16 even at a distance of 195 m from the VSP well. The updated interpretation differed from the original interpretation in that detailed imaging of the reef slope and an accurate correlation to the geological well results were achieved. The integrated geophysical/geological interpretation resulted in the decision that it was not economically feasible to whipstock the VSP well.

In conclusion, it seems evident that interpretive processing resulted in a greater understanding of the processing of the VSP data by the merging of the interpretation and processing procedures. The interpretive processing displays were used in the integrated geophysical/geological interpretations to further the knowledge about the subsurface in each of the case studies. The method of integrated geophysical/geological interpretation which previously primarily dealt with surface seismic and geological data has been further developed to include VSP data (Hinds et al., 1994c).